Harmful Algae
March 2021, Volume 103 Pages 102026 (12p.)
https://doi.org/10.1016/j.hal.2021.102026
https://archimer.ifremer.fr/doc/00687/79946/

Molecular networking as a novel approach to unravel toxin diversity of four strains of the dominant *Dinophysis* species from French coastal waters

Sibat Manoella [1, *], Réveillon Damien [1], Antoine Chloé [1, 2], Carpentier Liliane [1], Rovillon Georges-Augustin [1], Sechet Veronique [1], Bertrand Sophie [2, 3]

[1] Ifremer, Dyneco, Phycotoxins Laboratory, F-44000 Nantes, France
[2] Université de Nantes, MMS, EA 2160, Nantes, France
[3] ThalassOMICS Metabolomics Facility, Plateforme Corsaire, Biogenouest, Nantes, France

* Corresponding author : Manoella Sibat, email address : manoella.sibat@ifremer.fr

damien.reveillon@ifremer.fr ; chloe.antoine27@yahoo.fr ; liliane.carpentier@ifremer.fr ; Georges.Augustin.Rovillon@ifremer.fr ; veronique.sechet@ifremer.fr ; samuel.bertrand@univ-nantes.fr

Abstract :

Some species of the genus Dinophysis contain Diarrhetic shellfish Poisoning (DSP) toxins and are the main threat to shellfish farming in Europe including France. Dinophysis species are known to produce two families of bioactive lipophilic toxins: (i) okadaic acid (OA) and their analogues dinophysistoxins (DTXs) and (ii) pectenotoxins (PTXs). Only six toxins (OA, DTX1, DTX2, DTX3, PTX1 and PTX2) regulated by the European Union Legislation (EC No. 15/2011; 3) are routinely monitored using targeted chemical analysis by liquid chromatography coupled to mass spectrometry (LC-MS/MS) while toxic species of Dinophysis produce many other analogues. To tentatively identify unknown toxin analogues, a recent approach (Molecular Networking, MN) was used based on fragmentation data obtained by untargeted high resolution mass spectrometry (HRMS). An optimization of the data-dependent LC-HRMS/MS acquisition conditions was conducted to obtain more informative networks. The MN was applied to provide an overview of the chemical diversity of four strains belonging to three major Dinophysis species isolated from French coastal waters (D. acuta, D. caudata and the “D. acuminata complex” species D. acuminata and D. sacculus). This approach highlighted species-specific chemical patterns and also that Dinophysis chemical diversity is largely unexplored. Using MN allowed to identify directly known toxins and their relationship between species of Dinophysis, leading to the discovery of five new putative PTX analogues.

Graphical abstract

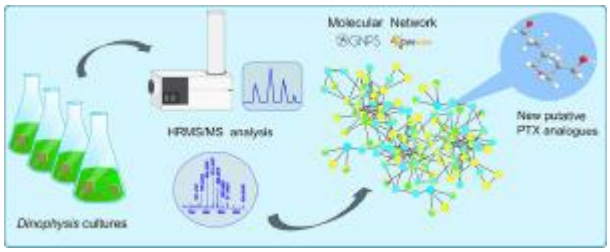

Highlights

► Molecular network revealed the presence of five new putative analogues of PTXs. ► Parameters optimization is essential to generate confident molecular networks. ► A molecular network was constructed to study *Dinophysis* toxin diversity. ► Molecular network highlighted characteristic profile for each *Dinophysis* species. ► Results suggest that *Dinophysis* chemical diversity is still largely unexplored.

Keywords : HRMS, Fragmentation, Molecular networking, Toxins, Dinophysis

1. Introduction

Dinoflagellates of the genus *Dinophysis* are the most prominent producers of Diarrhetic shellfish Poisoning (DSP) toxins which have an impact on public health and marine aquaculture worldwide (Yasumoto et al., 1980; Yasumoto et al., 1985; Reguera et al., 2014) In fact, a few hundred cells of toxic *Dinophysis* per liter may be sufficient to cause gastrointestinal illnesses in humans (Diarrhetic Shellfish Poisoning, DSP) generated by the consumption of contaminated shellfish (Yasumoto et al., 1980). In France, shellfish could become toxic even when *Dinophysis* was observed at concentration <100 cells per liter (Belin et al., 2020). The toxins produced by *Dinophysis* have been classified into two families of lipophilic compounds composed of: (i) a linear polyether group with okadaic acid (OA) and their analogues the dinophysistoxins (DTXs) and (ii) polyether macrolide toxins named pectenotoxins (PTXs). OA and DTXs have been shown to be potent phosphatase inhibitors (Bialojan and Takai, 1988), a property which can cause inflammation of the intestinal tract and diarrhea (Terao et al., 1986). On the opposite, PTXs have been demonstrated to be much less toxic *via* the oral route and to not induce diarrhea (Miles et al., 2004a). Even though PTXs are less toxic orally and do not cause diarrhea, they are lethal to mice by intraperitoneal injection, which is why that were regulated in the first place.

Since 1983, recurrent blooms of *Dinophysis* are observed in France by the phytoplankton and phycotoxin monitoring network (REPHY) that have caused regular closures for the professional's shellfish farming activity (Belin et al., 2020). Therefore, the economic, social and health issues associated with *Dinophysis* require additional studies to improve the knowledge of this dinoflagellate (e.g. its distribution, toxin profiles).

According to the thirty years of REPHY data (Belin et al., 2020), *Dinophysis sacculus* and *D. acuminata* have been identified as the main species responsible for toxic episodes on the French coasts. Although seasonal, the presence of *D. acuta, D. caudata, D. fortii, and D.*

tripos has been also recorded. Furthermore, a recent study (Séchet et al., 2021) confirmed the identification of the dominant "*D. acuminata* complex "= *D. sacculus and D. acuminata*) and the three species of *Dinophysis* (*D. acuta*, *D. caudata*, *D. tripos* from various sites of the French coastal waters, including the English Channel, the Bay of Biscay (Atlantic Ocean) and the Mediterranean Sea by combining genetic, morphological and toxin profile analyses. The term "*D. acuminata* complex" has been introduced for the co-occurring species *D. acuminata, D. sacculus, D. ovum and D. pavillardii* which are difficult to discriminate by morphology (Lassus and Bardouil, 1991). In Séchet et *al.*, (Séchet et al., 2021) the analyses by liquid chromatography coupled to low resolution tandem mass spectrometry (LC-LRMS/MS) of *Dinophysis* cultures revealed species-conserved toxin profiles irrespective of the geographical origin (Atlantic Ocean or Mediterranean Sea) in *D. acuta* , *D.caudata* and *D. tripos* and interestingly two distinct toxin profiles within the *D.acuminata*-complex. Furthermore, numerous studies confirmed the important biodiversity and variation of toxin profiles (chemodiversity) worldwide for the genus *Dinophysis* (Reguera et al., 2012) (for review, and references therein).

Targeted chemical analyses by LC-LRMS/MS are routinely used for the monitoring survey of regulated toxins (OA, DTX1, DTX2, DTX3, PTX1 and PTX2) in shellfish and to determine toxin profiles in microalgae. However, this approach is not suitable to highlight unknown toxin analogues, thus impairing the possibility to get a more general overview of existing toxins. Thanks to recent developments in mass spectrometry, it is nowadays possible to analyze MS^2 data obtained from an untargeted way by liquid chromatography coupled to high resolution mass spectrometry (LC-HRMS/MS) (e.g. using data-dependent MS/MS acquisition mode) (Wolfender et al., 2019).

The introduction of Molecular Networking (MN) (Guthals et al., 2012) allows to compare large scale data-dependent MS/MS spectra to highlight spectral similarities related to

compound structural similarities (Wan et al., 2002). This dereplication approach appears as a powerful tool to further identify unknown compound based on MS fragmentation information (Yang et al., 2013; Pinto et al., 2014; Wang et al., 2016; Fox Ramos et al., 2019). This approach was also recently used to study the chemical diversity of toxin-producer microalgae such as *Pseudo-nitzchia multistriata* (Fiorini et al., 2020) and *Prorocentrum lima* (Wu et al., 2020). Nevertheless, before obtaining informative networks, it is mandatory to optimize data-dependent LC-HRMS acquisition conditions (Olivon et al., 2017b).

To generate MN, several strategies have been recently developed (Yang et al., 2013; Olivon et al., 2017a; Olivon et al., 2018). In this study, a feature based with three major steps was used : (i) MZmine 2 for LC-MS data processing (Pluskal et al., 2010), (ii) the Global Natural Product Social Molecular Networking (GNPS) platform (Aron et al., 2020) to generate the feature based MN (FBMN) and (iii) Cytoscape (Shannon et al., 2003) designed for complex network analysis and visualization of large dataset.

To our knowledge, in this study, MN was applied for the first time to toxin-producing genus *Dinophysis* using untargeted LC-HRMS/MS. The aim was to provide a global overview of the chemical diversity of four strains belonging to three major *Dinophysis* species isolated from French coastal waters (*D. acuta, D. caudata and "D. acuminata* complex"). This approach allowed to identify directly known compounds and their relationship between species of *Dinophysis*, leading to the discovery of five potential new PTX analogues.

2. Materials and Methods

2.1. Isolation and cultures of *Dinophysis*

Seawater samples were collected from various locations on the French coasts during blooms of *Dinophysis,* at a depth of 1 m using a Niskin type flask.

Dinophysis sacculus (IFR-DSA-01Th) was isolated from the Mediterranean Sea (Thau Lagoon) in December 2015, *Dinophysis acuta* (IFR-DAC-01Ar) from the Atlantic Ocean at the entrance of the Arcachon Bay in August 2017. The two other strains, *Dinophysis caudata* (IFR-DCA-01Ke) and *Dinophysis acuminata* (IFR-DAU-01Ke), were isolated from the Atlantic Ocean at Douarnenez (Kervel) in October 2017 and May 2018, respectively. These organisms were identified by morphological and molecular biology (Séchet et al., 2021).

To ensure its growth, *Dinophysis* deploys a specific mixotrophic diet with a system of co-cultures of three organisms (Myung Gil Park et al., 2006). Cultures of the ciliate *Mesodinium rubrum* (Mr-DK2009, Acc. Number MG018339) from Helsingør Harbor (Denmark), fed the cryptophyte *Teleaulax amphioxeia* (AND-A0710) from Huelva (Spain), which were periodically given to *Dinophysis* as prey. Full details on culture conditions can be found in Séchet et al.,(Séchet et al., 2021).

2.2. Reagents and chemicals

LC-MS grade methanol, formic acid (98% purity) and ammonium formate were purchased from Sigma Aldrich GmbH (Steinheim, Germany). Water was deionized and purified at 18 MΩ cm^{-1} through a Milli-Q integral 3 system (Millipore, France). For HRMS, methanol, acetonitrile and high purity water were purchased from LC-MS Optima Fisher chemical (Illkirch, France).

Certified calibration solutions of OA, DTX1, DTX2 and PTX2 were purchased from the National Research Council Canada (NRC-CNRC, Halifax, Canada). As specified in the NRC-CNRC certificate of analysis, PTX2b and PTX2c were present as a non-certified standard in the PTX2 solution. The non-certified standard C8-diol ester of OA was purchased from Cifga (Lugo, Spain).

2.3. Sample preparation

A volume of 50 mL of each *Dinophysis* culture was collected during the exponential phase and centrifuged at 3500×g, 4°C for 15 min. Supernatants were removed and cell pellets were extracted twice with 2.5 mL MeOH using an ultrasonic bath (Elma Schmidbauer GmbH, Singen, Germany) at 25 KHz during 15 min in sweep mode. Once cells were disrupted, the supernatants were collected and combined (5 mL) after centrifugation (3500×g, 4°C, 15 min). A fixed cell equivalent concentration of 30 000 cells/mL was used, to allow for the comparison of the molecular networks between strains. Therefore extracts with the lowest concentration were concentrated under Nitrogen at 40°C and re-suspended in MeOH. All the samples were filtered through a Nanosep MF 0.2 µm filter and stored at -20°C until LC-HRMS/MS analysis.

2.4. HRMS/MS analysis

UHPLC-HRMS/MS analyses were carried out with a UHPLC system (1290 Infinity II, Agilent technologies, CA, USA) coupled to a high resolution time-of-flight mass spectrometer (Q-Tof 6550 iFunnel, Agilent technologies, CA, USA) equipped with a Dual Jet Stream® electrospray ionization (ESI) interface operating in positive mode. Chromatographic separation was carried out on a reversed-phase C_{18} Kinetex column (100 Å, 1.7 µm, 100 × 2.1 mm, Phenomenex, LePecq, France) at 40 °C using a mobile phase composed of water (A) and 95% acetonitrile/water (B) both containing 5 mM ammonium formate and 50 mM formic acid. The flow rate was set at 0.4 mL min^{-1} and the injection volume 5 µL. Separation was achieved using the following mobile phase gradient: start at 5%B for 1 min and rise from 5% to 100% B in 10 min, held at 100% B for 3 min, return to the initial condition (5% B) in 0.5 min and a re-equilibration period (5% B) for 5.0 min. Mass spectral detection was carried out in Auto MS/MS mode in positive (ESI^+) ion acquisition. The MS and MS^2 acquisition were operated from *m/z* 100 to 1700. A ramped collision energy with a slope of 5, an offset of 2.5 and a narrow isolation width (~1.3 amu)

was applied to the precursor ions. The spectral parameters and precursor ions selection were evaluated by data dependent (**Table 1**). The final Auto MS/MS acquisition parameters were set as follow: a fragmentation intensity threshold at 1000 counts, an active exclusion precursor after 3 spectra during 0.2 min and with an acquisition scan rate fixed at 7 spectra per second for MS^1 and 21 sp s^{-1} for MS^2.

The conditions of the ESI source were set as follows: source temperature, 200 °C; drying gas, N_2; flow rate, 11 mL min^{-1}; sheath gas temperature, 350 °C; sheath gas flow rate, 11 mL min^{-1}; nebulizer, 45 psig; capillary voltage, 3.5 kV; nozzle voltage, 500 V. The instrument was daily mass calibrated using the Agilent tuning mix diluted in acetonitrile by 10. An additional calibration-check was carried out continuously over the entire run time using reference masses *m/z* 121.0509 (purine) and *m/z* 922.0099 (hexakis phosphazine) infused in the dual spray source at a constant flow of 1.5 µL min^{-1}. Acquisition was controlled by MassHunter software (version B07, Agilent Technologies, CA, USA).

2.5. MS^2 Data processing

Raw agilent files .d format were converted to .mzXML format with the MS-convert program of proteowizard 3.0 (Chambers et al., 2012). The converted data were treated with the software MZmine 2 (version 2.38) (Pluskal et al., 2010) to create a preprocessing workflow with a series of stages. The noise level for mass detection was set at 0. The chromatogram builder step was achieved using ADAP algorithm with a minimum scan time of 0.05 min, a *m/z* tolerance of 30 ppm, a minimum height of 1000 and a minimum group size of 5. The chromatograms were deconvoluted using Wavelets algorithm with a signal to noise (S/N) threshold set at 10, a minimum height at 1000, a coefficient area threshold of 15 and with a RT wavelet range from 0.01 to 0.02 min. Chromatograms were deisotoped with a RT tolerance of 0.05 min and peaks were aligned with a *m/z* tolerance of 30 ppm and RT tolerance of 0.08 min. The peak list was exported to .mgf file.

2.6. Generate Molecular Network (MN)

The molecular networks were created on the GNPS online web-platform (Wang et al., 2016). The parameters workflow were used with the following settings: MS^1 tolerance 1.0 Da, MS^2 tolerance 0.1 Da, cosine score of 0.7, minimum of 6 fragment ions, minimum cluster size of 1 without MS cluster (because MZmine 2 pretreatment was operated) and a TopK set at 1000. The MN created was visualized using Cytoscape software (version 3.7.2) (Shannon et al., 2003).

2.7. Elemental formula modelling of new compounds using ChemCalc

Determination of elemental formula was performed with ChemCalc, an open source software (Patiny and Borel, 2013). For each compound **10** to **14**, the measured accurate mass given by the MN was entered in the Molecular Formula Finder application. To increase the relevance of the search, filters were pre-selected such as a $|\Delta ppm| < 10$ and the exact ranges of atoms were: C40–60 H60–100 O5–20 with (NH_4^+) (H^+), (Na^+) and (K^+) ionization.

3. Results and Discussion

Molecular networking methods are used to visualize the structural relationship between compounds belonging to a molecular family (Guthals et al., 2012). As the molecules are grouped according to their spectral similarities, an optimization of the MS^2 acquisition parameters was first proceeded to generate a more informative MN.

3.1. Optimization of MS^2 acquisition

The optimization of data acquisition was focused on maximising (i) the number of known toxins from *Dinophysis* species. and (ii) the diversity of fragmented precursor ions. This optimization was achieved using a mix of reference standards (OA, DTX1, DTX2, PTX2 and PTX2c) and a methanolic extract of *D. acuta* to better visualize any compounds that would be chemically close.

In a preliminary experiment (**Figure S1, Table 1**), the effect of lowering the fragmentation intensity threshold (IT) had been evaluated. An IT of 1000 was set for data acquisition as it will ultimately increase the chemical diversity explored by molecular networking including toxins.

3.1.1. Effect of scan rate acquisition (sp s^{-1}) and exclusion time (ET, min) on MS/MS spectra of known toxins using a mix of standard

Two criteria were explored namely the exclusion time (ET) for precursor ion selection (0, 0.5 and 0.05 min) along with the acquisition scan rate (from 1 to 7 sp s^{-1}). In each of the 21 corresponding methods, the presence of MS/MS spectra within the raw data (.mgf) was monitored for all toxins in each formed adduct: the protonated ion $[M+H]^+$, the ammonium adduct $[M+NH_4]^+$ and the sodium adduct $[M+Na]^+$ (**Table 2**). A specific attention to isobaric analogues was taken, which means that the ability of the methods to acquire MS/MS spectra for both OA and DTX2 and for both PTX2 and PTX2c was carefully checked.The results were presented in **Figure 1**.

The dot plot (**Figure 1**) indicates for each of the 21 methods, the number of MS/MS spectra that were acquired from the precursor ions corresponding to the three adducts. The MS/MS spectra of ammonium $[M+NH_4]^+$ and sodium $[M+Na]^+$ adducts of PTX2 were markedly more abundant ($n \geq 10$) especially at ET = 0 and 0.05 min. Overall (except for DTX2), MS/MS acquisition mostly occurred on $[M+Na]^+$ and $[M+NH_4]^+$ while the $[M+H]^+$ precursor ions either required higher acquisition scan rates or were never fragmented for PTX2 and PTX2c analogues, probably as a result of their low intensity in the HRMS full scan spectra (**Figure S2**).

Without any exclusion time (ET = 0 min), at least one of the three adducts was not fragmented, independently of the acquisition scan rate. A high ET (0.5 min) led to an improved number of fragmented adducts for OA and DTX1.The impact of this parameter was

234 particularly important for isobaric toxins such as OA/DTX2 and PTX2/PTX2c, because the
235 first eluted analogue may affect the selection of the second for fragmentation. Formerly, the
236 fragmentation of the first eluted compound, may exclude the fragmentation of other closely
237 eluted isobaric compounds. This happened for OA/DTX2 whose RT difference was 0.28 min.
238 In fact, the exclusion for 0.5 min after the scan of the $[M+Na]^+$ adduct of OA led to the
239 absence of MS/MS spectra for the isobaric $[M+Na]^+$ adduct of DTX2. In contrast, this was not
240 observed for PTX2/PTX2c because the retention time difference (0.85 min) was greater than
241 0.5 min. Therefore, a MS scan rate between 3 to 7 sp s^{-1} (and the corresponding MS^2
242 acquisition scan rate between 9 to 21 sp s^{-1}) was chosen for further investigations, to obtain a
243 maximum of fragmented toxin precursor ions.

244 **3.1.2. Final optimisation of exclusion time (ET) and MS acquisition scan rate for both**
245 **improved toxin fragmentation and chemical diversity coverage using a *Dinophysis***
246 **extract**

247 The results of the previous experiment showed that an exclusion time of 0.5 min improved the
248 diversity of precursor ions but could impair the detection of isobaric compounds (e.g.
249 OA/DTX2). Therefore, the ET needs to be further adjusted, between 0.05 and 0.5 min, to
250 enhance the fragmentation of all compounds, including toxins isomers with a low delta
251 retention time. Three new ET (0.1, 0.2 and 0.3 min) were evaluated at five acquisition scan
252 rate (3 to 7 sp s^{-1}) with an IT set at 1000 cps, yielding 15 different methods. On the one hand,
253 the number of unique precursors ions (**Figure 2a**) and on the other hand, the number of MS^2
254 spectra related to targeted toxins (**Figure 2b**) were compared to find the optimal conditions.
255 To ensure the fragmentation of the toxins of interest, the *m/z* of the different ions species of
256 the toxins (**Table 2**) were specified as "Preferred ions" in each Auto MS/MS method. Indeed,
257 precursors defined as "Preferred"on the Preferred/excluded parameters on **Table 1**, are always
258 considered before other potentially qualifying precursors.

As expected, an increase of both MS acquisition scan rate and ET, provided a better coverage of the chemical diversity of the methanolic extract of *D. acuta*, as reflected by the higher number of unique precursors (>1200) (**Figure 2a**). On the opposite, more MS² spectra (>50) related to targeted toxins were acquired at lower ET (0.1 min) (**Figure 2b**). Thus a compromise had to be done for optimal DDA parameters. An ET set at 0.2 min after 3 spectra with an acquisition scan rate fixed at 7 spectra per second allowed to obtain a large number of precursors ions (>1400) with 60 MS² spectra related to the referenced toxins.

The results of the experiments allowed us to find the optimal parameters (**Table 1**) to observe both a maximum number of compounds (>1400) as well as a maximum of fragmented referenced toxins (>50). Olivon et al., (2017b) also highlighted the influence of fragmentation parameters but on plant natural extracts the exclusion criteria seems to have a deleterious effect on MN. Despite the results of their study, their recommendation was to re-optimize the fragmentation parameters in particular the exclusion criteria. Therefore, this first step was essential to generate molecular networks with high confidence for the rest of our study.

3.2. Exploring the chemical diversity of *Dinophysis* using molecular networking

A molecular network (MN) was constructed from the alignment of MS² spectra to one another. The nodes correspond to the *m/z* of precursor ions. Nodes are connected by edges (lines) based on a similarity score called the “cosine score” (Wan et al., 2002) where the thickness of the edges corresponds to the strength of the MS² spectral similarities. The molecules with similar fragmentation patterns grouped in the same cluster. Indeed, molecular families tend to cluster together within these networks. The optimal parameters obtained allowed us to acquire suitable MS² spectra with a suitable number of fragments (6 ions minimum) to generate reliable molecular networks of four strains of *Dinophysis*.

283 Here, the feature-based MN (FBMN) (**Figure 3**) was constructed using methanolic extracts of
284 four strains of *Dinophysis* (*D. acuta, D. acuminata, D. sacculus and D. caudata*) on which
285 LC-HRMS/MS profiles were subjected to an optimized workflow using MZmine 2 software,
286 prior to generate FBMN with the GNPS platform. MZmine 2 software provides a complete
287 set of stages for the feature detection (peak picking, in particular with the presence of isobaric
288 compounds) and to get semi-quantitative information.
289 The entire MN is composed of 3048 nodes with 28791 connections and contains about ten
290 major clusters, twenty small clusters and 1140 single nodes. The pie chart function was used
291 to have a semi-quantitative color coding of nodes according to the strains: *D. acuta* was
292 represented in red, *D. acuminata* in yellow, *D. caudata* in green and *D. sacculus* in blue.
293 Exploration of the *Dinophysis* MN (**Figure 3**) allows to find clusters corresponding to only
294 one species of *Dinophysis*, for example cluster (3) was associated to *D. acuminata* while
295 cluster (4) to *D. caudata*. These species-clusters could appear as chemotaxonomy marker of
296 *Dinophysis* and require more chemical investigations beyond the scope of the current study.
297 In addition, this MN seems to show that these two *Dinophysis* species possess a larger
298 detected chemical diversity. Intriguingly, nodes related to *D. acuta* are much more dispersed
299 in the network, most of them being singletons (lonely nodes). Nodes were subjected to
300 dereplication using the GNPS database (Yang et al., 2013; Wang et al., 2016) and no
301 consistent annotation was found. This reflects the current lack of knowledge about the
302 metabolome of marine microalgae (Zendong et al., 2016) and especially *Dinophysis* species
303 where only 20 compounds were reported in the Dictionary of Natural Products (Chapman &
304 Hall 2020, CRC Press). Among those 20 compounds, only acuminolide A (Hwang et al.,
305 2014) – a 33-membered macrolide – was not considered similar to known toxins produced by
306 *Dinophysis.* This suggests that a huge effort is currently needed to study the chemical
307 diversity of toxic microalgae. Such knowledge is unfortunately mandatory to better explore

the chemotaxonomy of *Dinophysis,* and will require a higher level of identification than in Garcia-Portela et al., *(Garcia-Portela et al., 2018)*.

Highlighting the known toxins (**Table 2**, purple squares in the MN **Figure 3**) helped to capture the OA and PTX clusters and to reveal the presence of various related analogues. As the entire MN was very complex to fully interpret due to the lack of available chemical data about *Dinophysis* and keeping in mind the aim of this study, we decided to focus the interpretation on the toxin clusters.

3.3 Tracking toxin chemical diversity in Dinophysis using molecular networking

In the MN (**Figure 3**), two clusters corresponded to the toxins produced by the *Dinophysis* species studied here. This should allow to highlight the presence of new OA/DTX and PTX analogues.

3.3.1 Interpretation of the Okadaic acid (OA) cluster

The OA cluster was represented by only 5 nodes (Figure 3 cluster (2), **Figure 4**) but revealed the presence of OA in *D. sacculus, D. acuminata* and *D. acuta*. Compared to the standard (RT= 8.64 min), four nodes were easily identified at *m/z* 822.5009, 787.4626, 769.4526 and 751.4418 corresponding respectively to $[M+NH_4]^+$ and $[M+H-nH_2O]^+$ ions (n = 1 to 3). The pie chart of the nodes provided additional information regarding the relative abundance of OA in each of the three species. *Dinophysis acuminata* was clearly the species with the highest amount of OA compared to *D. acuta* and *D. sacculus.* These results are in agreement with a previous study (Séchet et al., 2021) where toxin profile of 30 clonal strains of *Dinophysis* cultures from French coastal waters were determined by quantitative LC-MS/MS. It was reported that the strains of *D. acuminata* contained only OA while *D. sacculus* produced OA and C9-diol ester of OA but in lower proportions. Interestingly, in the OA cluster, the last node with *m/z* 769.4530 at 9.60 min corresponded to *D. sacculus* and could be an already

described degradation product related to diol esters of OA (Suzuki and Quilliam, 2011; Sibat et al., 2018). Despite belonging to the same molecular family, as expected, no dinophysistoxins (DTX2 and/or DTX1) were associated to the OA cluster. To observe a clustering of OA, DTX2 and DTX1, a creation of a MN using a lower cosine score (0.4) was mandatory (**Figure S3**). However, only one node revealed the presence of DTX2 in *D. acuta* at *m/z* 787.4635 corresponding to $[M+H-H_2O]^+$ and one node for the standard of DTX1 at *m/z* 836.5196.

3.3.2 Interpretation of the pectenotoxin (PTX) cluster

As showed in cluster (1) on Figure 3 and in **Figure 5**, the PTX cluster contained 26 nodes corresponding to features present in three out of the four *Dinophysis* species (*D. sacculus*, *D. caudata* and *D. acuta*). The analysis of the cluster first resulted in the dereplication of three nodes by comparison with the standards: PTX2 (9.18 min), PTX2b (9.30 min) and PTX2c (10.04 min). It is noteworthy that our optimized strategy was successfully able to separate these 3 isobaric toxins in the MN. The relative areas of the metabolites allowed to have a rapid overview of the *Dinophysis* PTX profiles. The three species produced PTX2, PTX2b and PTX2c, although at traces for *D. acuta*. All other nodes from this cluster corresponded mainly to *D. sacculus* (12 nodes) and to a lesser extend to *D. caudata* (2 nodes) or to both species (6 nodes). Interestingly, *D. sacculus* was the most diversified PTX producer.

Further investigations were conducted to annotate the compounds corresponding to the PTX cluster (**Table 3.**). The nodes were grouped by their retention time and, the ions species were assigned to PTX analogues based on their molecular formula reported in the literature (Yasumoto et al., 1985; Sasaki et al., 1997; Sasaki et al., 1998; James et al., 1999; Suzuki et al., 2003; Miles et al., 2004a; Miles et al., 2004b; Miles et al., 2006; Suzuki et al., 2006). The mass differences (Δppm) between measured and exact theoretical masses were calculated to support the compound identification. Nine compounds (**1** to **9**) corresponding to 21 nodes in

the cluster were putatively identified as known analogues of PTXs with a very good mass error (Δ ppm < 2). The nodes corresponding to PTX2 (9.18 min) and PTX2c (10.04 min) were associated to the ammonium adduct $[M+NH_4]^+$ and the pseudo-molecular ions $[M+H-nH_2O]^+$ (n = 1 to 3). For PTX2b (9.30 min), only one node corresponding to $[M+NH4]^+$ was present. Therefore, we could assign all the nodes corresponding to compounds **5** to **7** (PTX2, PTX2b and PTX2c, respectively).

Compounds **1** to **4** corresponded to the molecular formula $C_{47}H_{70}O_{15}$ with the measured *m/z* corresponding to $[M+NH_4]^+$ and $[M+H-nH_2O]^+$ ions species. Due to the absence of reference standards, the possible identity of the isomers could be PTX1, PTX4, PTX8, PTX11, PTX11b, PTX11c or PTX13. According to the literature(Yasumoto et al., 1985; Sasaki et al., 1998; Miles et al., 2006; Suzuki et al., 2006), PTX1 and PTX4 are the oxidation products of the 43-methyl group of PTX2 that occur in the digestive glands of shellfish, thus they are not expected to be detected in *Dinophysis*. However, Krock et al.,(Krock et al., 2008) demonstrated that PTX1 was also detected in *D. acuminata* from the North Sea. Sasaki et al. (Sasaki et al., 1998), reported that PTX8 was found after an experimental auto-catalyzed acidic process of PTX4. This rearrangement was not observed in shellfish and although it is expected to be observed in the toxin-producing dinoflagellates, no PTX8 has been identified as a biosynthetic product from algae to date. In contrast, PTX11, PTX11b, PTX11c and PTX13 were isolated from *D. acuta* collected from New Zealand (Miles et al., 2006; Suzuki et al., 2006) while PTX11 was also reported in *D. acuminata* from North America (Hackett et al., 2009), *D. acuta* from European waters (Pizarro et al., 2008) and *D. tripos* from Argentina (Fabro et al., 2015). To our knowledge, no reported data were found about these analogues in *D. sacculus* and *D. caudata*. At this stage without reference standards, the possible identity of compounds **1** to **4** could be PTX1, PTX11, PTX11b, PTX11c and PTX13.

For the compounds **8** and **9,** nodes were assigned to $[M+NH_4]^+$ and $[M+H-H_2O]^+$ ions species, corresponding to the molecular formula $C_{47}H_{68}O_{14}$ of PTX12 and PTX14. According to the literature, PTX12 was isolated from *D. norvegica* and *D. acuta* from Norway (Miles et al., 2004b) and PTX14 was identified in *D. acuta* from New Zealand (Miles et al., 2006). In this study, PTX12 and PTX14 were putatively identified in *D. sacculus*, but further investigations with a reference material will be necessary to confirm this result.

Compounds **10** and **11** were tentatively associated to the $[M+NH_4]^+$ of the molecular formula $C_{47}H_{68}O_{16}$ but the mass errors (+28.1 and +41.1 ppm) were too large to be confidently considered as PTX6, PTX7 or PTX9. Miles et al. (Miles et al., 2006), reported that compounds at *m/z* 906 and 908 have been observed during LC-LRMS in a *D. acuta* sample from New Zealand but were not characterized due to their low abundance.

Very interestingly, compounds **12** to **14,** with respectively the measured *m/z* 806.4343, 908.5007 and 924.5309 were not associated to any known PTXs. Thus, they were considered as possible new unreported analogues.

3.4 Putative identification of the unknown compounds in the PTX cluster

3.4.1 Assignment of PTX product ions and comparison with MS^2 spectra of the unknown compounds

To tentatively elucidate the structure of the unknown compounds, HRMS/MS spectra of compounds **10** to **14** were compared to those of PTXs provided in previous studies (Suzuki et al., 2006; Krock et al., 2008; Suzuki and Quilliam, 2011). As observed in HR CID MS^2 spectra (**Figure 6**), the compounds **10**, **11**, **13** and **14** shared identical product ions with PTX1 and PTX11, in the *m/z* region of 700-900. As described in **Table 4,** the fragmentation of the $[M+NH_4]^+$ at *m/z* 892.5053, gives $[M+H]^+$ ion at *m/z* 875.4787, followed by a series of ions due to sequential water losses ($[M+H-nH_2O]^+$; n = 1 to 6). These series of water losses were

observed in the four HRMS/MS spectra, starting at two different stages depending on the compounds: (i) at *m/z* 857.4682 for **11** (Δ ppm = -2.08) and **13** (Δ ppm = +1.42) and (ii) at *m/z* 839.4576 for **10** (Δ ppm = -0.86) and **14** (Δ ppm = +0.34).

In accordance with the study by Suzuki et al. (Suzuki and Quilliam, 2011), a fragmentation pathway of PTX1/PTX11 (**Figure 7**) was proposed and fragment ions were assigned in **Table 4**. The HRMS/MS spectra of the compounds **10** to **14** showed prominent ions corresponding to those already reported for PTX at theoretical *m/z* 213.1121 ($C_{11}H_{16}O_4^+$) and *m/z* 195.1016 ($C_{11}H_{14}O_4^+$) assigned to the cleavage #01 + #02. The first cleavage observed (#01) is associated with the ring-opening of the macrocycle at the lactone site and followed by the fragmentation of B-ring (#02). Moreover, the combination of cleavages #01 with the opening of C-ring #03 followed by one or two water losses, gave the ions at *m/z* 293.1383 and *m/z* 275.1278 corresponding respectively to the elemental formula $C_{16}H_{20}O_5^+$ and $C_{16}H_{18}O_4^+$**.** These products ions were also observed in the spectra of the five compounds at low Δ ppm (<5 ppm).

According to the literature (Suzuki and Quilliam, 2011), the ion at *m/z* 551.2851 ($C_{29}H_{42}O_{10}^+$) resulting from cleavages #01 + #04, followed by three water losses corresponds to PTX11 spectrum. Interestingly, this set of four ions was observed in HRMS/MS spectra of compounds **10** to **14** with a low Δ ppm (<5 ppm), suggesting that this part of the structure is conserved between the five compounds.

All these fragmentations give additional information on the structure of the new analogues but unfortunately NMR studies will be required to complete their elucidation.

3.4.2 Possible Elemental formula of the new compounds

The determination of possible elemental formula of compounds **10** to **14** was performed using ChemCalc software(Patiny and Borel, 2013). The range of the measured accurate mass found for the compounds **10** to **14** was similar to the range of the theoretical accurate mass of the

known PTXs (**Table 3**). The assumption of a similar number of unsaturations was presumed from the similar molecular size and the common part of the structure of the analogues compared to PTX11. Therefore, for modelling the elemental formula of the unknown compounds a range from 7 to 16 unsaturations was chosen in ChemCalc. The proposed elemental formula generated by ChemCalc was listed in **Table 5**. For each compound, the elemental formula with the lowest mass difference and the most likely number of unsaturations was highlighted in grey ($C_{50}H_{75}O_{13}$ for compound 10, $C_{48}H_{72}O_{15}$ for 11, $C_{42}H_{60}O_{14}$ for 12, $C_{47}H_{70}O_{16}$ for 13 and $C_{48}H_{74}O_{16}$ for 14).

4. Conclusion

In this study, Molecular Networking was applied as a novel approach, to provide a more complete and structured overview of the toxin diversity produced by four major strains of *Dinophysis* isolated from French coastal waters (*D. acuminata*, *D. sacculus*, *D. acuta* and *D. caudata*). An optimization of the fragmentation parameters with a focus on the exclusion criteria and MS acquisition scan rate, allowed us to observe both a maximum of compounds as well as a maximum of fragmented referenced toxins to finally obtain an informative MN. The example presented here, clearly highlighted the importance of LC-HRMS/MS FBMN due to the high number of isobaric toxins in the data. Exploration of the MN pointed out a characteristic toxin profile for each *Dinophysis* strain and revealed the presence of five new putative analogues of PTXs: three analogues in *D. sacculus,* one in *D. caudata* and one which was common between *D. caudata* and *D. sacculus*.

Further investigations of HRMS/MS spectra in positive ionization were carried out to tentatively elucidate the structure of the unknown compounds. Relevant information was provided by the comparison of MS^2 spectra of PTX11 with the new analogues suggesting that a part of the PTX11 structure was conserved between the five compounds. Compound

isolation and NMR studies are however mandatory to propose the full structures of the newly reported analogues.

Acknowledgments:

The authors would like to acknowledge the colleagues from Ifremer coastal laboratories for tracking and sampling *Dinophysis*: A. Duval and A. Terre-Terrillon (LER Bretagne Occidentale), M. Perrière-Rumebe and C. Meteigner (LER Arcachon), E. Abadie and C. Hubert (LER Languedoc Roussillon). The authors acknowledge funding from IFREMER through REMODIF project. The authors acknowledge the technical ThalassOMICS facility of the Corsaire platform, Biogenouest.

Conflict of interest

The authors declare no conflict of interest.

Author Contributions:

M.S., V.S., D.R. and S.B. participate to the conceptualization and the coordination of the study. M.S. and G.R. conducted the LC-MS/MS data analysis, L.C. and V.S. contributed to establishing and maintaining *Dinophysis* clonal cultures; C.A., M.S., D.R. and S.B. participated to the data curation, MS contribute to writing—original draft preparation, all the authors contributed to writing—review and editing the paper. MS obtained the funding of the study.

References

Aron, A.T., Gentry, E.C., McPhail, K.L., Nothias, L.-F., Nothias-Esposito, M., Bouslimani, A., Petras, D., Gauglitz, J.M., Sikora, N., Vargas, F., van der Hooft, J.J.J., Ernst, M., Kang, K.B., Aceves, C.M., Caraballo-Rodríguez, A.M., Koester, I., Weldon, K.C., Bertrand, S., Roullier, C., Sun, K., Tehan, R.M., Boya P, C.A., Christian, M.H., Gutiérrez, M., Ulloa, A.M., Tejeda Mora, J.A., Mojica-Flores, R., Lakey-Beitia, J., Vásquez-Chaves, V., Zhang, Y.,

481 Calderón, A.I., Tayler, N., Keyzers, R.A., Tugizimana, F., Ndlovu, N., Aksenov, A.A.,
482 Jarmusch, A.K., Schmid, R., Truman, A.W., Bandeira, N., Wang, M., Dorrestein, P.C., 2020.
483 Reproducible molecular networking of untargeted mass spectrometry data using GNPS.
484 Nature protocols 15(6), 1954-1991.
485 Belin, C., Soudant, D., Amzil, Z., 2020. Three decades of data on phytoplankton and
486 phycotoxins on the French coast: Lessons from REPHY and REPHYTOX. Harmful Algae,
487 101733.
488 Bialojan, C., Takai, A., 1988. Inhibitory effect of a marine-sponge toxin, okadaic acid, on
489 protein phosphatases. Biochem journal 256, 283-290.
490 Chambers, M.C., Maclean, B., Burke, R., Amodei, D., Ruderman, D.L., Neumann, S., Gatto,
491 L., Fischer, B., Pratt, B., Egertson, J., Hoff, K., Kessner, D., Tasman, N., Shulman, N.,
492 Frewen, B., Baker, T.A., Brusniak, M.Y., Paulse, C., Creasy, D., Flashner, L., Kani, K.,
493 Moulding, C., Seymour, S.L., Nuwaysir, L.M., Lefebvre, B., Kuhlmann, F., Roark, J., Rainer,
494 P., Detlev, S., Hemenway, T., Huhmer, A., Langridge, J., Connolly, B., Chadick, T., Holly,
495 K., Eckels, J., Deutsch, E.W., Moritz, R.L., Katz, J.E., Agus, D.B., MacCoss, M., Tabb, D.L.,
496 Mallick, P., 2012. A cross-platform toolkit for mass spectrometry and proteomics. Nat
497 Biotechnol 30(10), 918-920.
498 Fabro, E., Almandoz, G.O., Ferrario, M.E., Hoffmeyer, M.S., Pettigrosso, R.E., Uibrig, R.,
499 Krock, B., 2015. Co-occurrence of Dinophysis tripos and pectenotoxins in Argentinean shelf
500 waters. Harmful Algae 42, 25-33.
501 Fiorini, F., Borgonuovo, C., Ferrante, M.I., Bronstrup, M., 2020. A Metabolomics
502 Exploration of the Sexual Phase in the Marine Diatom Pseudo-nitzschia multistriata. Mar
503 Drugs 18(6).

504 Fox Ramos, A.E., Evanno, L., Poupon, E., Champy, P., Beniddir, M.A., 2019. Natural
505 products targeting strategies involving molecular networking: different manners, one goal.
506 Natural product reports 36(7), 960-980.
507 Gaillard, S., Le Goic, N., Malo, F., Boulais, M., Fabioux, C., Zaccagnini, L., Carpentier, L.,
508 Sibat, M., Reveillon, D., Sechet, V., Hess, P., Hegaret, H., 2020. Cultures of Dinophysis
509 sacculus, D. acuminata and pectenotoxin 2 affect gametes and fertilization success of the
510 Pacific oyster, Crassostrea gigas. Environmental pollution 265(Pt B), 114840.
511 Garcia-Portela, M., Reguera, B., Sibat, M., Altenburger, A., Rodriguez, F., Hess, P., 2018.
512 Metabolomic Profiles of Dinophysis acuminata and Dinophysis acuta Using Non-Targeted
513 High-Resolution Mass Spectrometry: Effect of Nutritional Status and Prey. Mar Drugs 16(5).
514 Guthals, A., Watrous, J.D., Dorrestein, P.C., Bandeira, N., 2012. The spectral networks
515 paradigm in high throughput mass spectrometry. Mol Biosyst 8(10), 2535-2544.
516 Hackett, J.D., Tong, M., Kulis, D.M., Fux, E., Hess, P., Bire, R., Anderson, D.M., 2009. DSP
517 toxin production de novo in cultures of Dinophysis acuminata (Dinophyceae) from North
518 America. Harmful Algae 8(6), 873-879.
519 Hwang, B.S., Kim, H.S., Yih, W., Jeong, E.J., Rho, J.R., 2014. Acuminolide A: structure and
520 bioactivity of a new polyether macrolide from dinoflagellate Dinophysis acuminata. Organic
521 letters 16(20), 5362-5365.
522 James, K.J., Bishop, A.G., Draisci, R., Palleschi, L., Marchiafava, C., Ferretti, E., Satake, M.,
523 Yasumoto, T., 1999. Liquid chromatographic methods for the isolation and identification of
524 new pectenotoxin-2 analogues from marine phytoplankton and shellfish. Journal of
525 chromatography. A 844(1-2), 53-65.
526 Krock, B., Tillmann, U., Selwood, A.I., Cembella, A.D., 2008. Unambiguous identification of
527 pectenotoxin-1 and distribution of pectenotoxins in plankton from the North Sea. Toxicon
528 52(8), 927-935.

529 Lassus, P., Bardouil, M., 1991. LE COMPLEXE "DINOPHYSIS ACUMINATA":
530 IDENTIFICATION DES ESPÈCES LE LONG DES CÔTES
531 FRANÇAISES. Cryptogamie, Algologie 12(1), 1-9.
532 Miles, C.O., Wilkins, A.L., Hawkes, A.D., Jensen, D.J., Selwood, A.I., Beuzenberg, V.,
533 Lincoln MacKenzie, A., Cooney, J.M., Holland, P.T., 2006. Isolation and identification of
534 pectenotoxins-13 and -14 from Dinophysis acuta in New Zealand. Toxicon 48(2), 152-159.
535 Miles, C.O., Wilkins, A.L., Munday, R., Dines, M.H., Hawkes, A.D., Briggs, L.R., Sandvik,
536 M., Jensen, D.J., Cooney, J.M., Holland, P.T., Quilliam, M.A., MacKenzie, A.L.,
537 Beuzenberg, V., Towers, N.R., 2004a. Isolation of pectenotoxin-2 from Dinophysis acuta and
538 its conversion to pectenotoxin-2 seco acid, and preliminary assessment of their acute
539 toxicities. Toxicon 43(1), 1-9.
540 Miles, C.O., Wilkins, A.L., Samdal, I.A., Sandvik, M., Petersen, D., Quilliam, M.A.,
541 Naustvoll, L.J., Rundberget, T., Torgersen, T., Hovgaard, P., 2004b. A Novel Pectenotoxin,
542 PTX-12, in Dinophysis Spp. and Shellfish from Norway. Chem. Res. Toxicology 17, 1423-
543 1433.
544 Myung Gil Park, Sunju Kim, Hyung Seop Kim, Geumog Myung, Yi Gu Kang, Yih, W., 2006.
545 First successful culture of the marine dinoflagellate Dinophysis acuminata. Aquatic Microbial
546 Ecology 45, 101-106.
547 Olivon, F., Elie, N., Grelier, G., Roussi, F., Litaudon, M., Touboul, D., 2018. MetGem
548 Software for the Generation of Molecular Networks Based on the t-SNE Algorithm. Anal
549 Chem 90(23), 13900-13908.
550 Olivon, F., Grelier, G., Roussi, F., Litaudon, M., Touboul, D., 2017a. MZmine 2 Data-
551 Preprocessing To Enhance Molecular Networking Reliability. Anal Chem 89(15), 7836-7840.

552 Olivon, F., Roussi, F., Litaudon, M., Touboul, D., 2017b. Optimized experimental workflow
553 for tandem mass spectrometry molecular networking in metabolomics. Anal Bioanal Chem
554 409(24), 5767-5778.
555 Patiny, L., Borel, A., 2013. ChemCalc: a building block for tomorrow's chemical
556 infrastructure. Journal of chemical information and modeling 53(5), 1223-1228.
557 Pinto, J.P., Machado, R.S., Xavier, J.M., Futschik, M.E., 2014. Targeting molecular networks
558 for drug research. Front Genet 5, 160.
559 Pizarro, G., Paz, B., Franco, J.M., Suzuki, T., Reguera, B., 2008. First detection of
560 Pectenotoxin-11 and confirmation of OA-D8 diol-ester in Dinophysis acuta from European
561 waters by LC–MS/MS. Toxicon 52(8), 889-896.
562 Pluskal, T., Castillo, S., Villar-Briones, A., Oresic, M., 2010. MZmine 2: modular framework
563 for processing, visualizing, and analyzing mass spectrometry-based molecular profile data.
564 BMC bioinformatics 11, 395.
565 Reguera, B., Riobo, P., Rodriguez, F., Diaz, P.A., Pizarro, G., Paz, B., Franco, J.M., Blanco,
566 J., 2014. Dinophysis toxins: causative organisms, distribution and fate in shellfish. Mar Drugs
567 12(1), 394-461.
568 Reguera, B., Velo-Suárez, L., Raine, R., Park, M.G., 2012. Harmful Dinophysis species: A
569 review. Harmful Algae 14, 87-106.
570 Sasaki, K., Satake, M., Yasumoto, T., 1997. Identification of the absolute configuration of
571 pectenotoxin-6, a polyether macrolide compound, by NMR spectroscopic method using a
572 chiral anisotropic reagent, phenylglycine methyl ester. Bioscience, biotechnology, and
573 biochemistry 61(10), 1783-1785.
574 Sasaki, K., Wright, J.L., Yasumoto, T., 1998. Identification and Characterization of
575 Pectenotoxin (PTX) 4 and PTX7 as Spiroketal Stereoisomers of Two Previously Reported
576 Pectenotoxins. J Org Chem 63(8), 2475-2480.

577 Séchet, V., Sibat, M., Billien, G., Carpentier, L., Rovillon, G.-A., Raimbault, V., Malo, F.,
578 Gaillard, S., Perrière-Rumebe, M., Hess, P., Chomérat, N., 2021. Characterization of toxin-
579 producing strains of Dinophysis spp. (Dinophyceae) isolated from French coastal waters, with
580 a particular focus on the D. acuminata-complex. Harmful Algae, 101974.
581 Shannon, P., Markiel, A., Ozier, O., Baliga, N.S., Wang, J.T., Ramage, D., Amin, A.,
582 Schwikowski, B., Ideker, T., 2003. Cytoscape: A Software Environment for Integrated
583 Models of Biomolecular Interaction Networks. Cold Spring Harbor Laboratory Press 13(11),
584 2498_2504.
585 Sibat, M., Garcia-Portela, M., Hess, P., 2018. First identification of a C9-diol-ester of okadaic
586 acid in Dinophysis acuta from Galician Rias Baixas (NW Spain). Toxicon.
587 Suzuki, T., Beuzenberg, V., Mackenzie, L., Quilliam, M.A., 2003. Liquid chromatography–
588 mass spectrometry of spiroketal stereoisomers of pectenotoxins and the analysis of novel
589 pectenotoxin isomers in the toxic dinoflagellate Dinophysis acuta from New Zealand. J.
590 Chromatogr. A 992(1–2), 141-150.
591 Suzuki, T., Quilliam, M.A., 2011. LC-MS/MS analysis of diarrhetic shellfish poisoning
592 (DSP) toxins, okadaic acid and dinophysistoxin analogues, and other lipophilic toxins. Anal
593 Sci 27(6), 571-584.
594 Suzuki, T., Walter, J.A., LeBlanc, P., MacKinnon, S., Miles, C.O., Wilkins, A.L., Munday,
595 R., Beuzenberg, V., MacKenzie, A.L., Jensen, D.J., Cooney, J.M., Quilliam, M.A., 2006.
596 Identification of Pectenotoxin-11 as 34S-Hydroxypectenotoxin-2, a New Pectenotoxin
597 Analogue in the Toxic Dinoflagellate Dinophysis acuta from New Zealand. Chemical
598 research in toxicology 19, 310-318.
599 Terao, K., Ito, E., Yanagi, I., Yasumoto, T., 1986. Histopathological studies on experimental
600 marine toxin poisoning. I. ultrastructural changes in the small intestine and liver of suckling
601 mice induced by dinophysistoxin-1 and pectenotoxin-1 Toxicon 24(11-12), 1141-1151.

602 Wan, K.X., Vidavsky, l., and Gross, M.L., 2002. Comparing Similar Spectra: From
603 Similarity Index to Spectral Contrast Angle. Journal American society for mass spectrometry
604 13, 85-88.
605 Wang, M., Carver, J.J., Phelan, V.V., Sanchez, L.M., Garg, N., Peng, Y., Nguyen, D.D.,
606 Watrous, J., Kapono, C.A., Luzzatto-Knaan, T., Porto, C., Bouslimani, A., Melnik, A.V.,
607 Meehan, M.J., Liu, W.T., Crusemann, M., Boudreau, P.D., Esquenazi, E., Sandoval-Calderon,
608 M., Kersten, R.D., Pace, L.A., Quinn, R.A., Duncan, K.R., Hsu, C.C., Floros, D.J., Gavilan,
609 R.G., Kleigrewe, K., Northen, T., Dutton, R.J., Parrot, D., Carlson, E.E., Aigle, B.,
610 Michelsen, C.F., Jelsbak, L., Sohlenkamp, C., Pevzner, P., Edlund, A., McLean, J., Piel, J.,
611 Murphy, B.T., Gerwick, L., Liaw, C.C., Yang, Y.L., Humpf, H.U., Maansson, M., Keyzers,
612 R.A., Sims, A.C., Johnson, A.R., Sidebottom, A.M., Sedio, B.E., Klitgaard, A., Larson, C.B.,
613 P, C.A.B., Torres-Mendoza, D., Gonzalez, D.J., Silva, D.B., Marques, L.M., Demarque, D.P.,
614 Pociute, E., O'Neill, E.C., Briand, E., Helfrich, E.J.N., Granatosky, E.A., Glukhov, E., Ryffel,
615 F., Houson, H., Mohimani, H., Kharbush, J.J., Zeng, Y., Vorholt, J.A., Kurita, K.L.,
616 Charusanti, P., McPhail, K.L., Nielsen, K.F., Vuong, L., Elfeki, M., Traxler, M.F., Engene,
617 N., Koyama, N., Vining, O.B., Baric, R., Silva, R.R., Mascuch, S.J., Tomasi, S., Jenkins, S.,
618 Macherla, V., Hoffman, T., Agarwal, V., Williams, P.G., Dai, J., Neupane, R., Gurr, J.,
619 Rodriguez, A.M.C., Lamsa, A., Zhang, C., Dorrestein, K., Duggan, B.M., Almaliti, J., Allard,
620 P.M., Phapale, P., Nothias, L.F., Alexandrov, T., Litaudon, M., Wolfender, J.L., Kyle, J.E.,
621 Metz, T.O., Peryea, T., Nguyen, D.T., VanLeer, D., Shinn, P., Jadhav, A., Muller, R., Waters,
622 K.M., Shi, W., Liu, X., Zhang, L., Knight, R., Jensen, P.R., Palsson, B.O., Pogliano, K.,
623 Linington, R.G., Gutierrez, M., Lopes, N.P., Gerwick, W.H., Moore, B.S., Dorrestein, P.C.,
624 Bandeira, N., 2016. Sharing and community curation of mass spectrometry data with Global
625 Natural Products Social Molecular Networking. Nat Biotechnol 34(8), 828-837.

626 Wolfender, J.L., Nuzillard, J.M., van der Hooft, J.J.J., Renault, J.H., Bertrand, S., 2019.
627 Accelerating Metabolite Identification in Natural Product Research: Toward an Ideal
628 Combination of Liquid Chromatography-High-Resolution Tandem Mass Spectrometry and
629 NMR Profiling, in Silico Databases, and Chemometrics. Anal Chem 91(1), 704-742.
630 Wu, H., Chen, J., Peng, J., Zhong, Y., Zheng, G., Guo, M., Tan, Z., Zhai, Y., Lu, S., 2020.
631 Nontarget Screening and Toxicity Evaluation of Diol Esters of Okadaic Acid and
632 Dinophysistoxins Reveal Intraspecies Difference of Prorocentrum lima. Environ Sci Technol
633 54(19), 12366-12375.
634 Yang, J.Y., Sanchez, L.M., Rath, C.M., Liu, X., Boudreau, P.D., Bruns, N., Glukhov, E.,
635 Wodtke, A., de Felicio, R., Fenner, A., Wong, W.R., Linington, R.G., Zhang, L., Debonsi,
636 H.M., Gerwick, W.H., Dorrestein, P.C., 2013. Molecular networking as a dereplication
637 strategy. Journal of natural products 76(9), 1686-1699.
638 Yasumoto, T., Murata, A., Oshima, Y., Sano, M., Matsumoto, G.K., Clardy, J., 1985.
639 Diarretic shellfish toxins. Tetrahedron 41(6), 1019-1025.
640 Yasumoto, T., Sugawara, W., Fukuyo, Y., Oguri, H., Igarashi, T., Fujita, N., 1980.
641 Identification of Dinophysis fortii as the causative organism of diarrhetic shellfish poisoning
642 in the Tohoku district. Bulletin of the Japanese Society of Scientific Fisheries 46, 1405-1411.
643 Zendong, Z., Bertrand, S., Herrenknecht, C., Abadie, E., Jauzein, C., Lemee, R., Gouriou, J.,
644 Amzil, Z., Hess, P., 2016. Passive Sampling and High Resolution Mass Spectrometry for
645 Chemical Profiling of French Coastal Areas with a Focus on Marine Biotoxins. Environ Sci
646 Technol 50(16), 8522-8529.

647

648

649 **TABLES**

650 **Table 1.** Data dependent for QTOF 6550 Auto MS/MS acquisition parameters

Experiment	**Spectral parameters**		**Precursor selection**		**Preferred/excluded**		
	MS (spetra s^{-1})	MS/MS (spetra s^{-1})	Threshold (cps)	Exclusion time (min)	Precursor (*m/z*)	Δ ppm	prec type
Preliminary	3 to 5	9 to 15	2000 / 1000	0.05 / 0.5	na*	na	na
Intermediate	1 to 7	3 to 21	1000	0 / 0.05 / 0.5	na	na	na
Final	3 to 7	9 to 21	1000	0.1 / 0.2 / 0.3	876.5104 881.4658 805.4733 822.4998 827.4552	20	include
Optimized	7	21	1000	0.2	876.5104 881.4658 805.4733 822.4998 827.4552	20	include

651 *not applied

652

653 **Table 2**. List of monitored toxins in the mix: retention time (RT) and ions species

654 corresponding to the theoretical accurate mono-isotopic *m/z* of the three detected adducts.

Toxins	RT (min)	Molecular formula	Ions species (*m/z*)		
			$[M+H]^+$	$[M+NH_4]^+$	$[M+Na]^+$
OA	8.64	$C_{44}H_{68}O_{13}$	805.4733	822.4998	827.4552
DTX2	8.92	$C_{44}H_{68}O_{13}$	805.4733	822.4998	827.4552
DTX1	9.65	$C_{45}H_{70}O_{13}$	819.4889	836.5155	841.4709
PTX2	9.19	$C_{47}H_{70}O_{14}$	859.4838	876.5104	881.4658
PTX2c	10.04	$C_{47}H_{70}O_{14}$	859.4838	876.5104	881.4658

655

656

Table 3. List of the annotated compounds corresponding to the cluster of PTXs (**Figure 5**). The mass-to-charge ratio (*m/z*) values in the table correspond to the nodes (precursor ions). A putative assignment of the molecular formula and ions species was operated based on the PTX analogues reported in the literature. Mass differences (Δ ppm) were compared between measured and exact theoretical masses.

Compound	RT (min)	Measured *m/z*	Ions species	Molecular formula	Δ ppm	Putative Identity
1	8.50	892.5067	$[M+NH_4]^+$	$C_{47}H_{70}O_{15}$	+1.6	PTX1, PTX4, PTX8, PTX11,
		857.4686	$[M+H-H_2O]^+$		+0.5	PTX11b, PTX11c or PTX13
		839.4584	$[M+H-2H_2O]^+$		+0.9	
		821.4479	$[M+H-3H_2O]^+$		+1.0	
2	8.68	892.5057	$[M+NH_4]^+$	$C_{47}H_{70}O_{15}$	+0.5	PTX1, PTX4, PTX8, PTX11,
						PTX11b, PTX11c or PTX13
3	8.75	892.5061	$[M+NH_4]^+$	$C_{47}H_{70}O_{15}$	+0.9	PTX1, PTX4, PTX8, PTX11,
		857.4690	$[M+H-H_2O]^+$		+1.0	PTX11b, PTX11c or PTX13
		839.4583	$[M+H-2H_2O]^+$		+0.8	
4	8.95	892.5061	$[M+NH_4]^+$	$C_{47}H_{70}O_{15}$	+0.9	PTX1, PTX4, PTX8, PTX11,
		857.4683	$[M+H-H_2O]^+$		+0.1	PTX11b, PTX11c or PTX13
5	9.18	876.5116	$[M+NH_4]^+$	$C_{47}H_{70}O_{14}$	+1.4	PTX2
		841.4738	$[M+H-H_2O]^+$		+0.5	
		823.4633	$[M+H-2H_2O]^+$		+0.7	
6	9.30	876.512	$[M+NH_4]^+$	$C_{47}H_{70}O_{14}$	+1.8	PTX2b
7	10.04	876.5115	$[M+NH_4]^+$	$C_{47}H_{70}O_{14}$	+1.3	PTX2c
		841.4736	$[M+H-H_2O]^+$		+0.4	
		823.4634	$[M+H-2H_2O]^+$		+0.8	
		805.4535	$[M+H-3H_2O]^+$		+1.7	
8	9.55	874.4958	$[M+NH_4]^+$	$C_{47}H_{68}O_{14}$	+1.9	PTX12 or PTX14
9	10.27	874.4964	$[M+NH_4]^+$	$C_{47}H_{68}O_{14}$	+1.9	PTX12 or PTX14
		839.4589	$[M+H-H_2O]^+$		+1.2	
10	9.43	906.5103	$[M+NH_4]^+$	$C_{47}H_{68}O_{16}$	+28.1	PTX6, PTX7 or PTX9

11	9.85	906.5218	$[M+NH_4]^+$	+41.1	
12	8.12	806.4343			Unreported compound
13	8.58	908.5007			Unreported compound
14	9.28	924.5309			Unreported compound

662

663

Table 4. Assignment of product ions observed in positive HRMS/MS spectra (**Figure 6**) of the unknown compounds associated to the PTX cluster, corresponding to cleavages reported in **Figure 7** and according to Suzuki et al (Suzuki and Quilliam, 2011) for PTX1 and PTX11.

	PTX1		**PTX11**		**Compound 10**		**Compound 11**		**Compound 12**		**Compound 13**		**Compound 14**	
Cleavage	Formula	theoretical (m/z)	Formula	theoretical (m/z)	measured (m/z)	Δ ppm	measured (m/z)	Δ ppm	measured (m/z)	Δ ppm	measured (m/z)	Δ ppm	measured (m/z)	Δ ppm
Parent ion	$C_{47}H_{73}NO_{15}^+$	892.5053	$C_{47}H_{73}NO_{15}^+$	892.5053	906.5103	/	906.5218	/	806.4343	/	908.5007	/	924.5309	/
	$C_{47}H_{70}O_{15}^+$	875.4787	$C_{47}H_{70}O_{15}^+$	875.4787	n.d*	/	n.d	/	n.d	/	n.d	/	n.d	/
	$C_{47}H_{68}O_{14}^+$	857.4682	$C_{47}H_{68}O_{14}^+$	857.4682	n.d	/	857.4664	-2.08	n.d	/	857.4694	1.42	n.d	/
	$C_{47}H_{66}O_{13}^+$	839.4576	$C_{47}H_{66}O_{13}^+$	839.4576	839.4569	-0.86	839.4574	-0.26	n.d	/	839.4579	0.34	839.4579	0.34
	$C_{47}H_{64}O_{12}^+$	821.4471	$C_{47}H_{64}O_{12}^+$	821.4471	821.4434	-4.45	821.4472	0.18	n.d	/	821.4473	0.30	821.4457	-1.65
	$C_{47}H_{62}O_{11}^+$	803.4365	$C_{47}H_{62}O_{11}^+$	803.4365	803.4350	-1.85	803.4369	0.51	n.d	/	803.4372	0.89	803.4359	-0.73
	$C_{47}H_{60}O_{10}^+$	785.4259	$C_{47}H_{60}O_{10}^+$	785.4259	785.4250	-1.18	785.4242	-2.20	n.d	/	785.4259	-0.03	785.4238	-2.70
	$C_{47}H_{58}O_9^+$	767.4154	$C_{47}H_{58}O_9^+$	767.4154	767.4135	-2.48	767.4138	-2.08	n.d	/	767.4151	-0.39	767.4121	-4.30
#01+#04	$C_{29}H_{42}O_{11}^+$	567.2800	$C_{29}H_{42}O_{10}^+$	551.2851	551.2854	0.54	551.2849	-0.36	n.d	/	551.2865	2.54	551.2866	2.72
	$C_{29}H_{40}O_{10}^+$	549.2694	$C_{29}H_{40}O_9^+$	533.2745	533.2752	1.30	533.2733	-2.27	533.2733	-2.27	533.2745	-0.02	533.2750	0.92
	$C_{29}H_{38}O_9^+$	531.2589	$C_{29}H_{38}O_8^+$	515.2639	515.2645	1.08	515.2639	-0.09	515.2618	-4.16	515.2640	0.11	515.2619	-3.97
	$C_{29}H_{38}O_8^+$	513.2483	$C_{29}H_{38}O_7^+$	497.2534	497.2514	-4.02	497.2523	-2.21	497.2529	-1.01	497.2538	0.80	497.2534	0.00
#01+#03	$C_{16}H_{22}O_6^+$	311.1489	$C_{16}H_{22}O_6^+$	311.1489	n.d	/	n.d	/	n.d	/	n.d	/	n.d	/
$-H_2O$	$C_{16}H_{20}O_5^+$	293.1383	$C_{16}H_{20}O_5^+$	293.1383	293.1389	2.05	293.1393	3.41	293.1380	-1.02	293.1397	4.78	293.1375	-2.73
$-2H_2O$	$C_{16}H_{18}O_4^+$	275.1278	$C_{16}H_{18}O_4^+$	275.1278	275.1265	-4.73	275.1277	-0.36	275.1278	0.00	275.1284	2.18	n.d	/
#01+#02	$C_{11}H_{16}O_4^+$	213.1121	$C_{11}H_{16}O_4^+$	213.1121	213.1121	-0.16	213.1127	2.65	213.1126	2.18	213.1131	4.53	213.1124	1.24
$-H_2O$	$C_{11}H_{14}O_3^+$	195.1016	$C_{11}H_{14}O_3^+$	195.1016	195.1013	-1.39	195.1017	0.66	195.1018	1.18	195.1017	0.66	195.1015	-0.36
$-2H_2O$	$C_{11}H_{12}O_2^+$	177.0910	$C_{11}H_{12}O_2^+$	177.0910	177.0913	1.66	177.0911	0.53	177.0911	0.53	177.0911	0.53	177.0905	-2.86

*n.d: non detected

668 **Table 5**. List of the proposed elemental formula with their corresponding number of

669 unsaturations generated by ChemCalc for the precursor ions annotated **10** to **14** in **Table 3**.

Compound	Ranking	Elemental formula	unsaturation	monoisotopicMass	Ions species	*m/z* theoretical	Δ ppm
Compound 10	01	$C_{50}H_{75}O_{13}$	13.5	883.5208	$[M+Na]^+$	906.5100	+0.3
906.5103	02	$C_{44}H_{72}O_{18}$	9	888.4719	$[M+NH_4]^+$	906.5057	+5.1
	03	$C_{45}H_{77}O_{18}$	7.5	905.5110	$[M+H]^+$	906.5183	-8.8
Compound 11	01	$C_{48}H_{72}O_{15}$	13	888.4871	$[M+NH_4]^+$	906.5209	+0.9
906.5218	02	$C_{45}H_{77}O_{18}$	7.5	905.5110	$[M+H]^+$	906.5183	+3.9
	03	$C_{51}H_{79}O_{11}$	12.5	867.5622	$[M+K]^+$	906.5254	-4.0
Compound 12	01	$C_{42}H_{60}O_{14}$	13	788.3983	$[M+NH_4]^+$	806.4321	2.7
806.4343	02	$C_{45}H_{67}O_{10}$	12.5	767.4734	$[M+K]^+$	806.4366	-2.8
	03	$C_{39}H_{65}O_{17}$	7.5	805.4222	$[M+H]^+$	806.4295	+6.0
	#04	$C_{41}H_{67}O_{14}$	8.5	783.4531	$[M+Na]^+$	806.4423	-9.9
Compound 13	01	$C_{47}H_{70}O_{16}$	13	890.4664	$[M+NH_4]^+$	908.5002	+0.5
908.5007	02	$C_{44}H_{75}O_{19}$	7.5	907.4903	$[M+H]^+$	908.4975	+3.5
	03	$C_{50}H_{77}O_{12}$	12.5	869.5415	$[M+K]^+$	908.5047	-4.4
Compound 14	01	$C_{48}H_{74}O_{16}$	12	906.4977	$[M+NH_4]^+$	924.5315	-0.7
924.5309	02	$C_{51}H_{81}O_{12}$	11.5	885.5728	$[M+K]^+$	924.5360	-5.5
	03	$C_{52}H_{75}O_{14}$	15.5	923.5157	$[M+H]^+$	924.5230	+8.6

670

Title of the figures

Figure 1. Dot plot representing the number of times (n) a precursor ion corresponding to toxins (OA, DTX1, DTX2, PTX2 and PTX2c) was fragmented depending on the acquisition scan rate (sp s^{-1}) and the exclusion time (ET, min). The fragmentation intensity threshold was set to 1000 counts, precursor ions were considered in a $\Delta m/z = 0.1$ and $\Delta RT = 0.2$ min windows. The size of the circle is proportional to the number of times the ions have been fragmented.

Figure 2: Final optimisation to evaluate the exclusion time (min) and the MS acquisition scan rate (sp s^{-1}) on the number of (**a**) unique precursor ions and (**b**) MS^2 spectra obtained for toxins.

Figure 3: Molecular network (MN) of four strains of *Dinophysis* species: *D. acuta* (in red), *D. acuminata* (in yellow), *D. caudata* (in green) and *D. sacculus* (in blue) including the standard toxins (purple squares around the nodes). MN was created with the following parameters: cosine score of 0.7, minimum of 6 common fragment ions and a TopK set at 1000. On each node, the pie chart highlights the relative peak area of each precursor ion in the raw LC-HRMS/MS profiles.

Figure 4: Okadaic acid (OA) cluster from the MN of the four *Dinophysis* species: *D. sacculus* (in blue), *D. acuminata* (in yellow) and *D. acuta* (in red), OA was not detected in *D. caudata*. Each node contained the *m/z* of the precursor ion and a pie chart showing the relative peak area of each precursor ion in the raw LC-HRMS/MS profiles. The standard toxins were highlighted by purple squares around the nodes. The retention times (in min) is indicated below each node.

Figure 5: Pectenotoxin (PTX) cluster from the MN of the four *Dinophysis* species: *D. acuta* (in red), *D. caudata* (in green) and *D. sacculus* (in blue), PTXs were not detected in *D. acuminata*. Each node contained the *m/z* of the precursor ion and a pie chart showing the

relative peak area of each precursor ion in the raw LC-HRMS/MS profiles. The standard toxins were highlighted by purple squares around the nodes. The retention times (in min) is indicated below each node. LC-HRMS chromatogram of PTX2 isobaric compounds is represented on the right.

Figure 6: HRMS/MS spectra of the putative new PTX analogues in *D. sacculus*, acquired in positive Auto MS/MS mode applying a ramped collision energy with a slope of 5, an offset of 2.5. MS/MS spectra corresponding to: **A**) compound **10** selecting *m/z* 906.5103 at 9.4 min, **B**) compound **11** selecting *m/z* 906.5218 at 9.8 min, **C**) compound **13** selecting *m/z* 908.5007 at 8.6 min and **D**) compound **14** with *m/z* 924.5309 at 9.3 min. Characteristic fragments of PTX were reported in red in the MS^2 spectra.

Figure 7: Proposed MS/MS fragmentation cleavages of PTX1/PTX11 in positive HRMS/MS analysis. Cleavages are the same as reported in Suzuki et al. (Suzuki and Quilliam, 2011). Assignment of fragment ions is reported in **Table 3**.

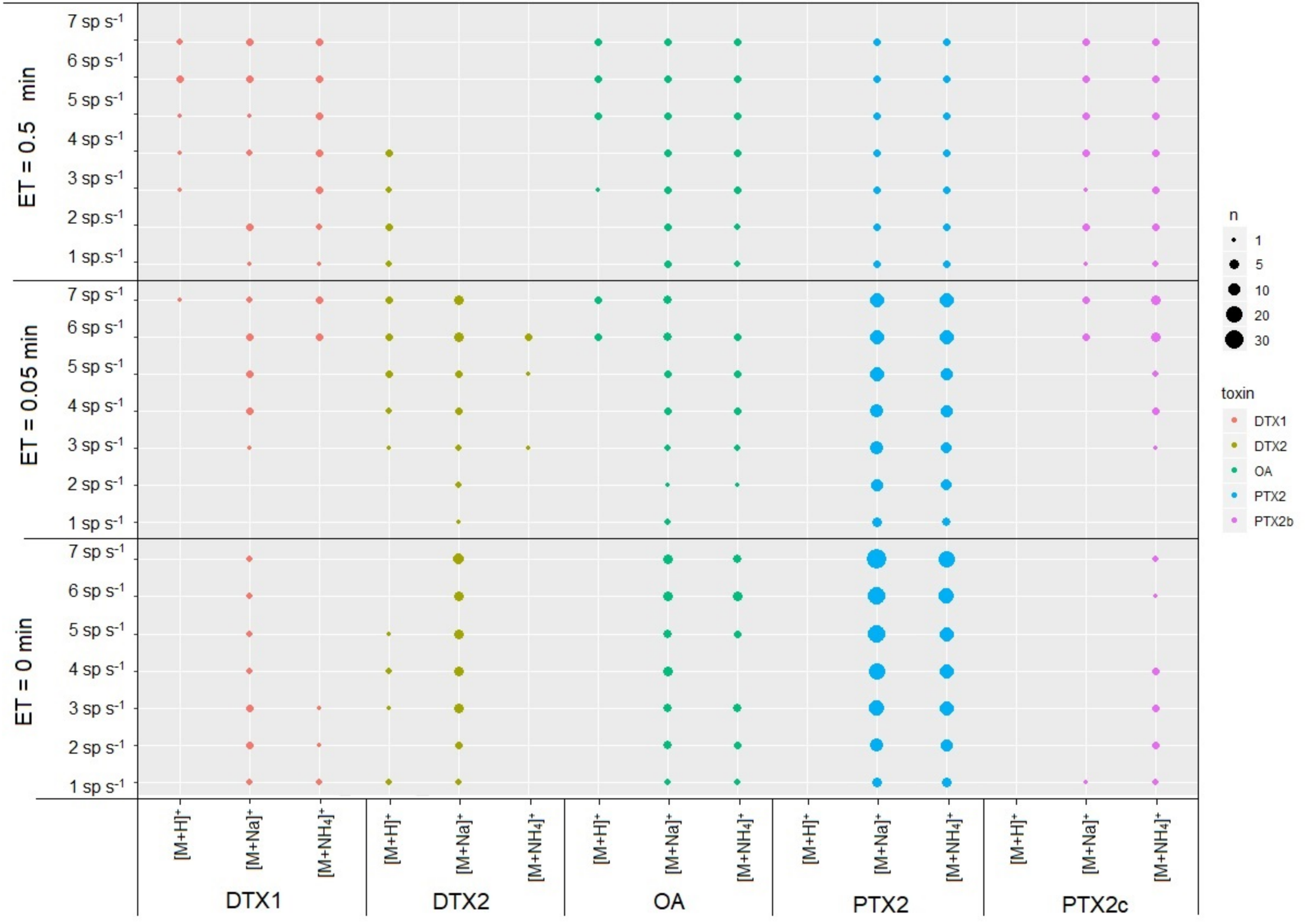
ET = 0.5 min
ET = 0.05 min
ET = 0 min
7 sp s-1
6 sp s-1
5 sp s-1
4 sp s-1
3 sp s-1
2 sp.s-1
1 sp.s-1
1 sp s-1
2 sp s-1
[M+H]+
[M+Na]+
[M+NH4]+
DTX1
DTX2
OA
PTX2
PTX2c
n
1
5
10
20
30
toxin
DTX1
DTX2
OA
PTX2
PTX2b

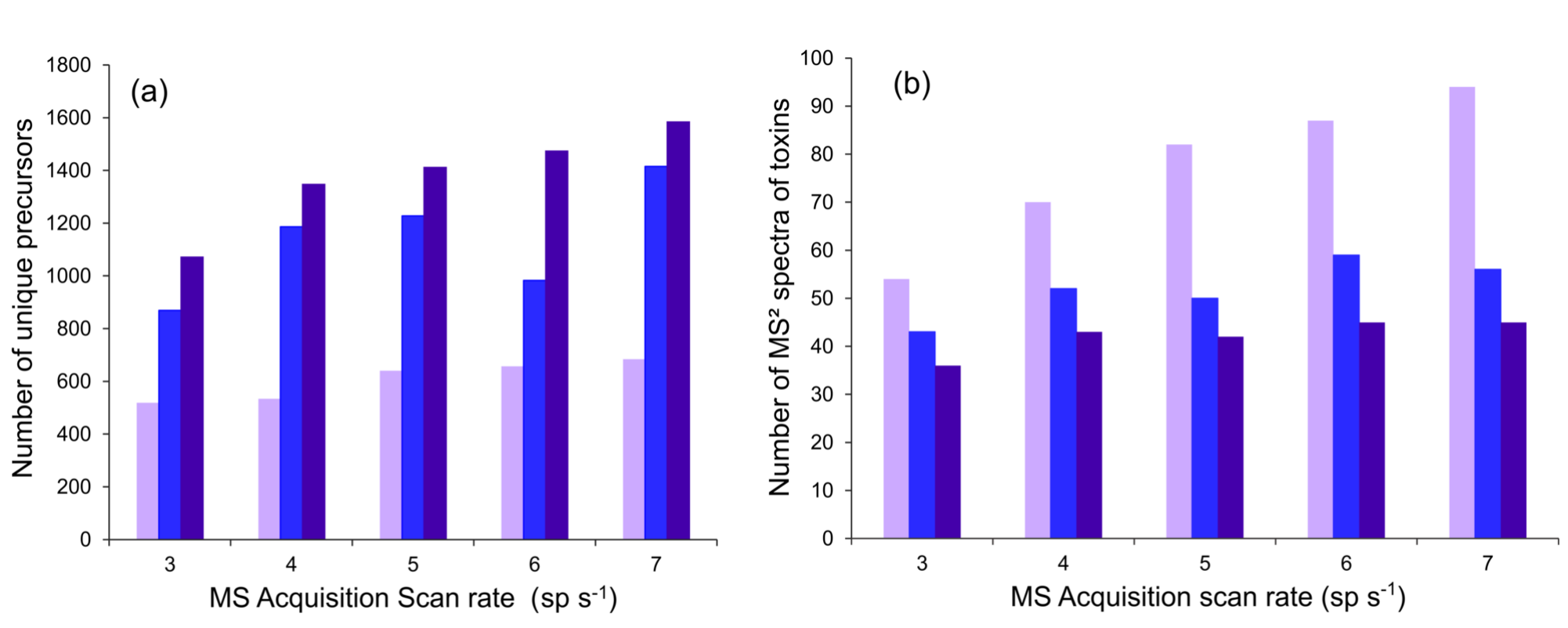
(a)
Number of unique precursors
1800
1600
1400
1200
1000
800
600
400
200
0
3
4
5
6
7
MS Acquisition Scan rate (sp s-1)
(b)
Number of MS² spectra of toxins
100
90
80
70
60
50
40
30
20
10
0
3
4
5
6
7
MS Acquisition scan rate (sp s-1)
Exclusion Time
0.1 min
0.2 min
0.3 min

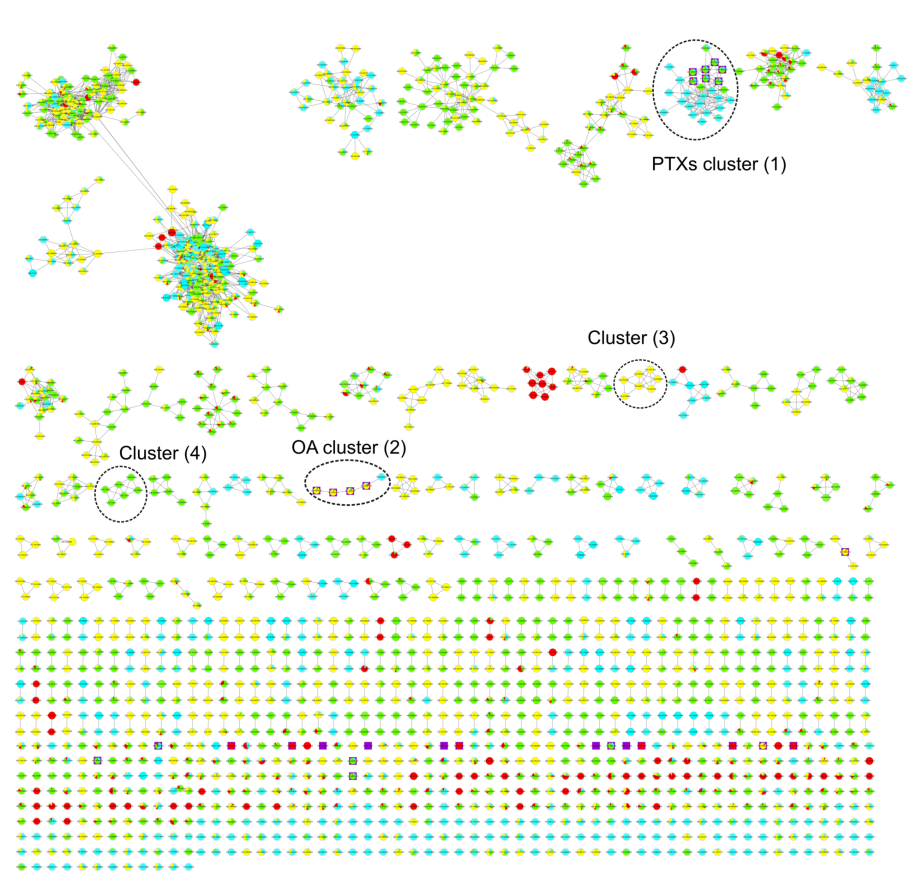
PTXs cluster (1)
Cluster (3)
Cluster (4)
OA cluster (2)

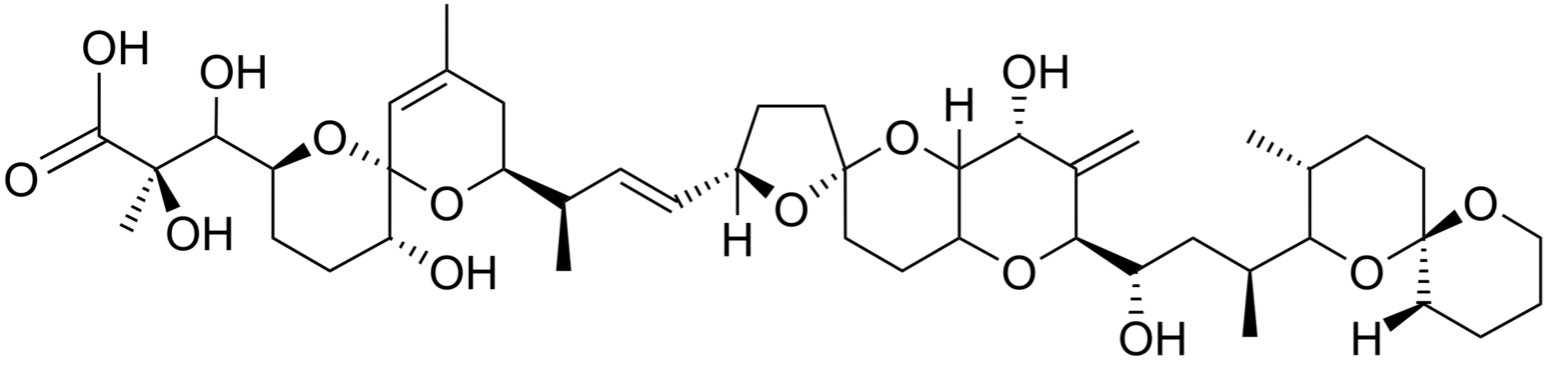

OA structure

769.4526
8.64
751.4418
8.64
787.4626
8.64
822.5009
8.64
769.4530
9.60
OA standard
D. sacculus
D. acuminata
D. acuta

PTX2 structure

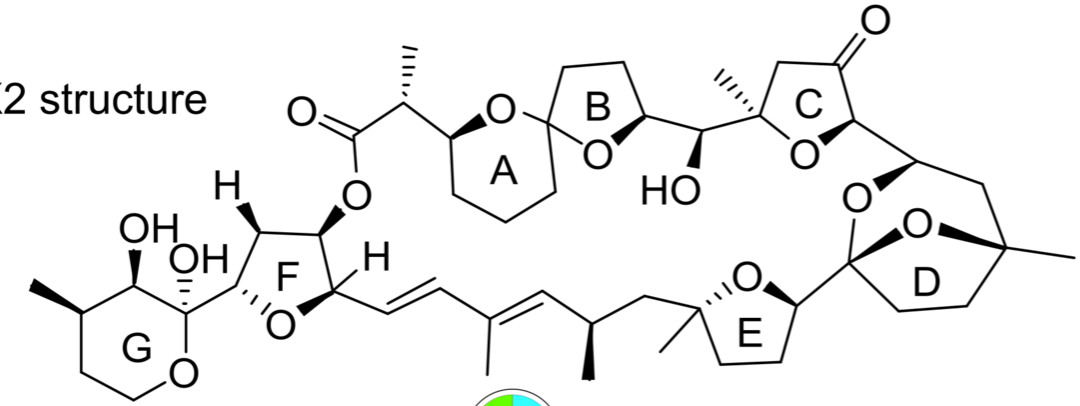

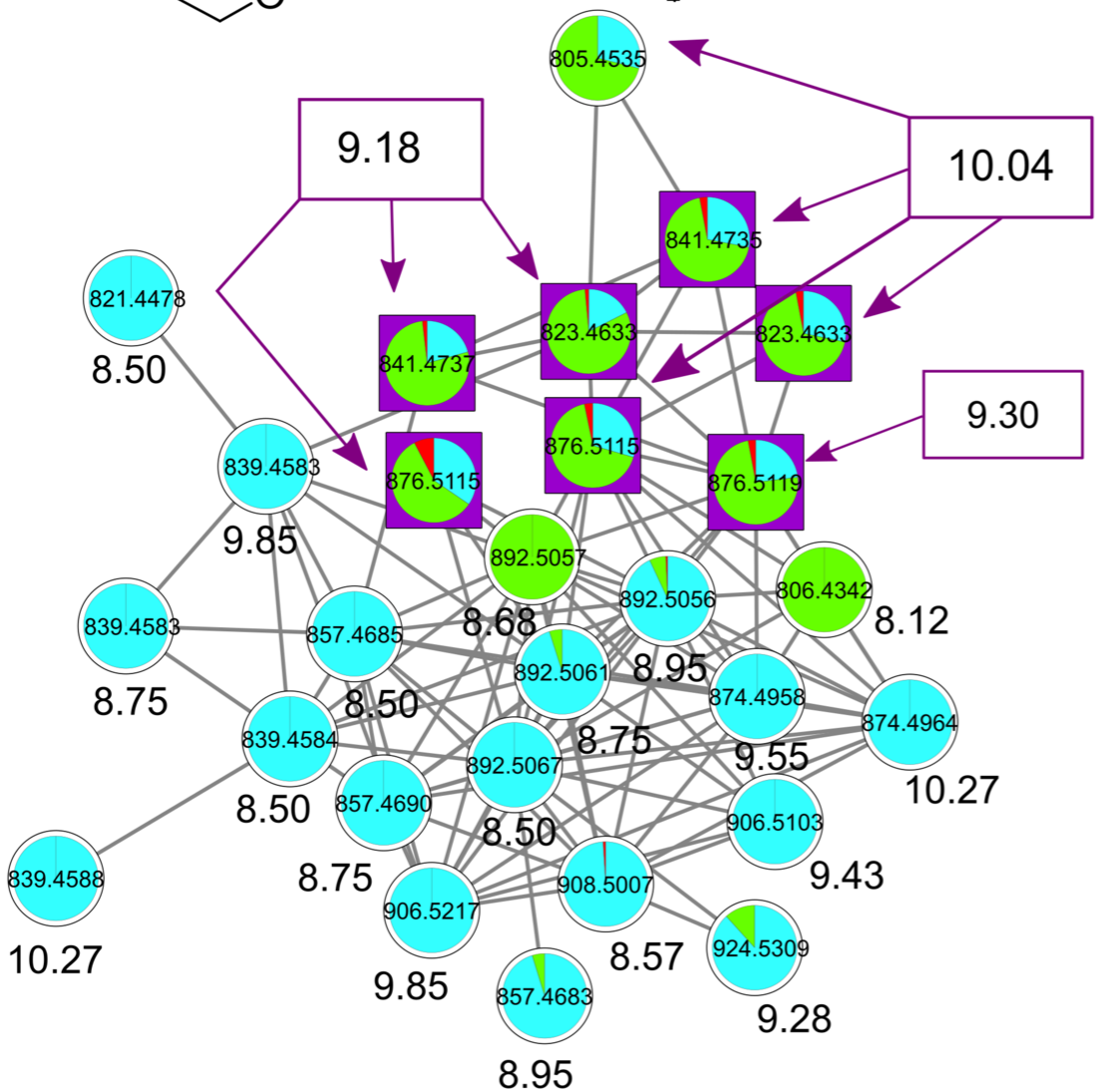

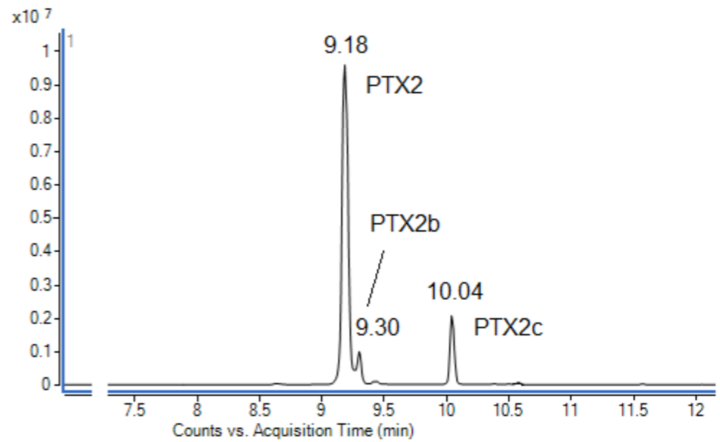

PTX2 standards

D. sacculus

D. caudata

D. acuta

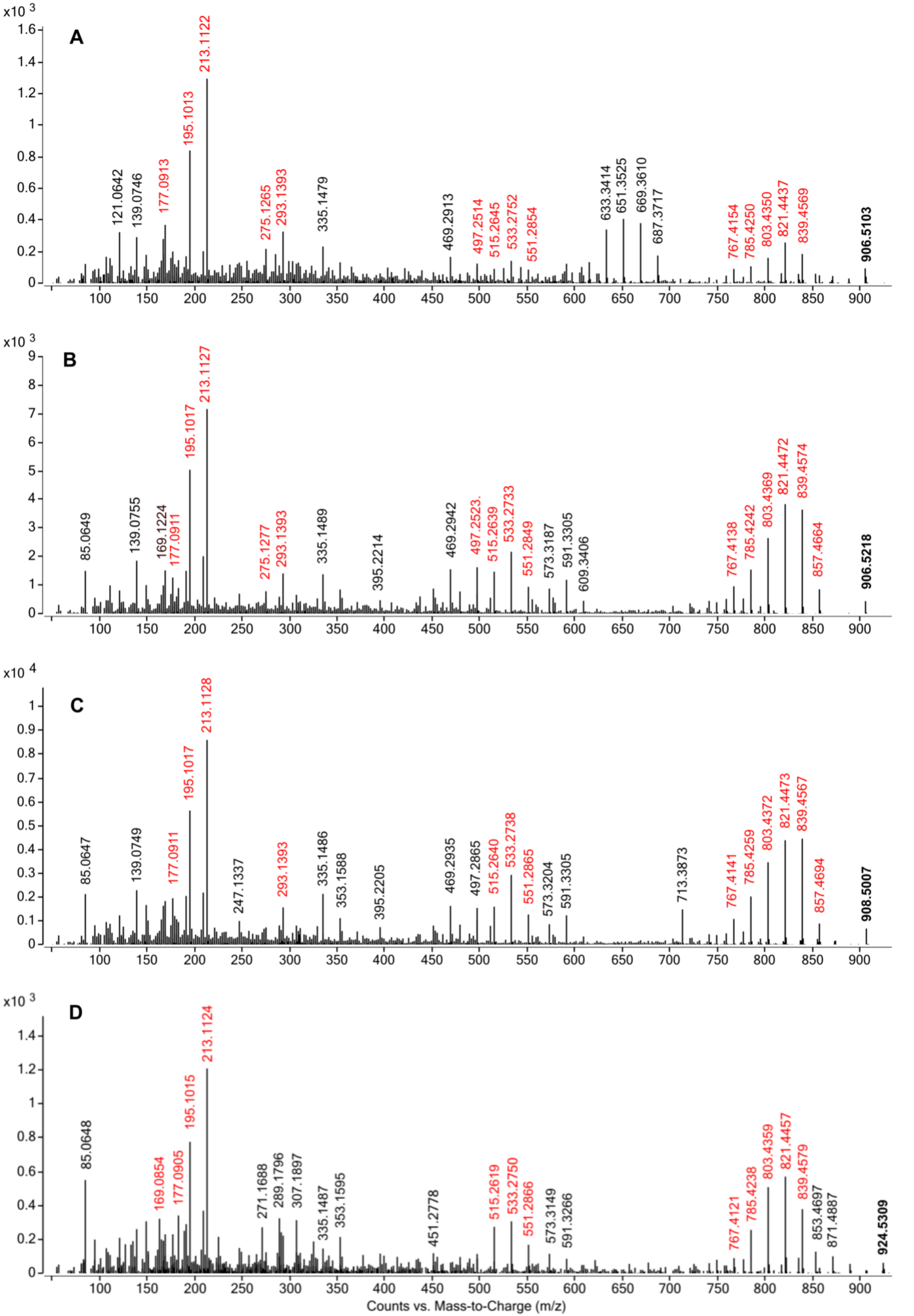
A
x10 3
121.0642
139.0746
177.0913
195.1013
213.1122
275.1265
293.1393
335.1479
469.2913
497.2514
515.2645
533.2752
551.2854
633.3414
651.3525
669.3610
687.3717
767.4154
785.4250
803.4350
821.4437
839.4569
906.5103
B
x10 3
85.0649
139.0755
169.1224
177.0911
195.1017
213.1127
275.1277
293.1393
335.1489
395.2214
469.2942
497.2523.
515.2639
533.2733
551.2849
573.3187
591.3305
609.3406
767.4138
785.4242
803.4369
821.4472
839.4574
857.4664
906.5218
C
x10 4
85.0647
139.0749
177.0911
195.1017
213.1128
247.1337
293.1393
335.1486
353.1588
395.2205
469.2935
497.2865
515.2640
533.2738
551.2865
573.3204
591.3305
713.3873
767.4141
785.4259
803.4372
821.4473
839.4567
857.4694
908.5007
D
x10 3
85.0648
169.0854
177.0905
195.1015
213.1124
271.1688
289.1796
307.1897
335.1487
353.1595
451.2778
515.2619
533.2750
551.2866
573.3149
591.3266
767.4121
785.4238
803.4359
821.4457
839.4579
853.4697
871.4887
924.5309
Counts vs. Mass-to-Charge (m/z)

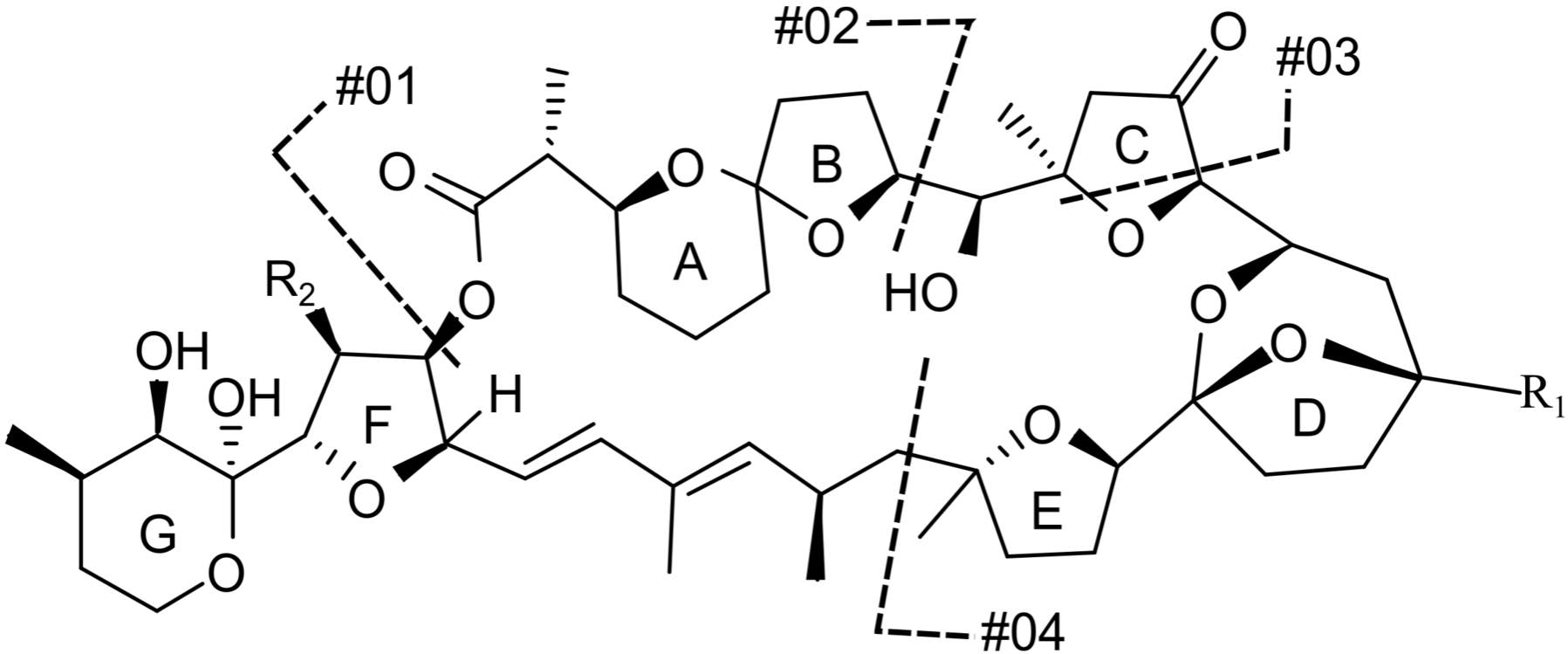

	R_1	R_2
PTX1	OH	H
PTX11	H	OH

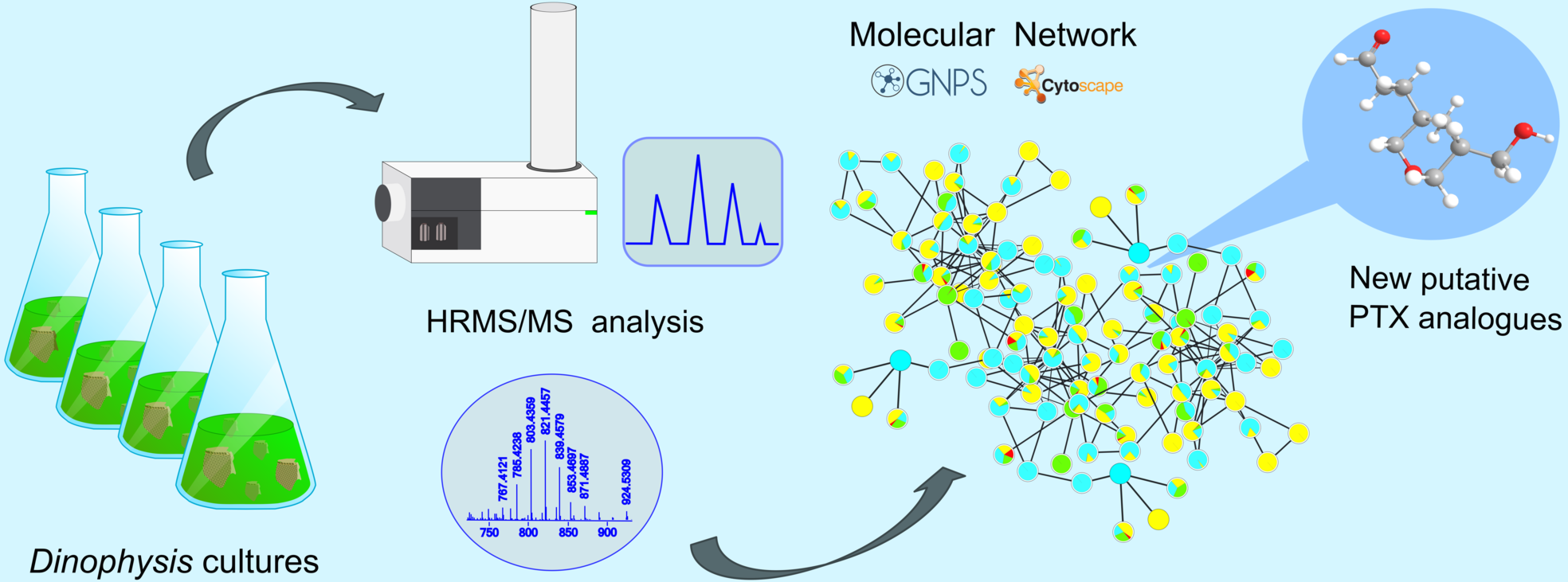
Molecular Network
GNPS
Cytoscape
HRMS/MS analysis
767.4121
785.4238
803.4359
821.4457
839.4579
853.4697
871.4887
924.5309
750
800
850
900
New putative
PTX analogues
Dinophysis cultures